

## **Mechanisms of compression in well graded saprolitic soils**

**I. Rocchi<sup>a,1</sup> & M.R. Coop<sup>b</sup>**

<sup>a</sup> Department of Civil, Chemical, Environmental and Materials Engineering,  
University of Bologna, Viale Risorgimento 2, 40316, Bologna, Italy, formerly City  
University of Hong Kong

<sup>b</sup> Department of Architecture and Civil Engineering, City University of Hong Kong,  
83, Tat Chee Avenue Kowloon Tong, Hong Kong S.A.R.

<sup>1</sup> Corresponding author: Tel: +39 051 2090523  
Fax: +39 051 2093527  
irene.rocchi3@unibo.it

**Abstract**

Soils originating from weathering processes present considerable heterogeneity in their composition, which can make it difficult to analyse their behaviour in a systematic way. For the granitic saprolites discussed in this paper, based on a trend between soil density and weathering degree, there appears to be two different domains of behaviour, a granular domain and a clay matrix one, according to the degree of weathering reached. Recognition of these domains can reduce the apparent scatter of data for the engineering behaviour of weathered soils. A number of one-dimensional compression tests are presented for saprolitic soils from Hong Kong having different weathering degrees. In addition, isotropic and one-dimensional compression tests from the literature on other saprolites from Hong Kong and around the world, were reanalysed and used to identify possible trends in the mechanisms of compression for these two domains. From practical considerations, the trends considered were between compressibility and common engineering grading descriptors. An attempt was also made to provide the physical explanations behind the behaviour observed and the particle breakage was investigated in detail, both from a quantitative and qualitative point of view. It was found that the values of relative breakage (Hardin, 1985), for a same stress level, might be very similar for soils having different compressibility values and different initial gradings. The maximum particle size, rather than the amount of fines in a mixture, may be a better predictor for differences in compressibility and breakage.

**Key words**

Weathering, well graded soil, saprolite, compression, breakage

## Introduction

Soils originating from the weathering of non-sedimentary rocks do not undergo any sorting in their grading, typically resulting in well graded particle size distributions. Weathering may influence the composition of soil in one or more aspects, e.g. particle size, particle size distribution, mineralogy or particle morphology, all of which influence its mechanical behaviour. As the heterogeneity of the weathering processes adds to the difficulties encountered studying these soils, it would be desirable to establish which parameters are more likely to influence the basic engineering behaviour, and this paper considers the compressibility.

While the mechanisms of compression in uniform sands are well understood (e.g. Coop & Lee 1993), some uncertainties still remain in describing the behaviour of binary mixtures (e.g., Thevanayagam & Mohan 2000). For example, there is agreement (e.g., Lade & Yamamuro 1997, Carrera et al. 2011) that with increasing fines the mechanisms of compression evolve from those of a granular soil to those of a fine grained soil, the minimum value of compressibility and lowest location of the normal compression line in the volume: stress plane being at an intermediate or transitional mixture. However, it is less clear what this value of fines should be for different soils (Zuo & Baudet 2015) and how the nature of the fines influences the mechanics of compression. The approach proposed by Thevanayagam & Mohan (2000) suggests using the traditional definition of void ratio at the two mixture extremes and an inter-granular or inter-fine void ratio for intermediate cases, depending on whether the mechanics are fines or coarse grain dominated, but it remains rather subjective when to use one definition or the other as the transitional fines content is highly variable and difficult to predict (Zuo & Baudet 2015). This type of approach may also only be used if the particle size distribution is binary and there is sufficient separation of the two grading sizes.

The plasticity of the fines may also influence the role that they have, requiring modification of the definition of the inter-granular or skeletal void ratio (e.g. Thevanayagam et al. 2002).

However, considerable work is still needed to shed light on the behaviour of well graded soils. Recent studies focusing on the behaviour of very well graded soils with fractal gradings gave contradictory results. Altuhafi & Coop (2011) found that no breakage could be observed after one-dimensional compression in soils having an initial fractal grading, despite the considerable volumetric change observed. They put forward the hypothesis that particle rearrangement and abrasion at the grain contacts could be the mechanisms responsible for the plastic volumetric strain. This appeared to be confirmed when analysing the particle morphology, which showed some changes in particle roughness but no major splitting. Minh & Cheng (2013) could reproduce qualitatively the experimental results published by Altuhafi & Coop (2011), using DEM models that assumed no particle breakage. From the work of Coop et al. (2004) it was found that in shearing a stable grading was only reached at shear strains in excess of a few thousand percent, and so it is possible that even an initially fractal grading may undergo breakage during shear, as Miao & Airey (2013) found, although their “fractal” grading was a limited one that did not include fines.

According to the international standards, upon which many national classification systems are based, including GEO (1988) in Hong Kong, a weathered rock can be classified based on the degree of chemical decomposition undergone by its minerals. In these classification systems six grades are identified, from fresh rock to residual soil. The weathered grades of granitic saprolites having a soil-like appearance are Highly Decomposed Granite (HDG), Completely Decomposed Granite (CDG) and Residual Soil (RS), which correspond to grades IV to VI. In Hong Kong, to this general classification, a description of the “consistency” of the soil is added, e.g. “weak”.

Baynes & Dearman (1978) proposed a qualitative trend between the weathering degree and the soil in-situ bulk density, based on data collected by Lumb (1962), and suggested a distinction between a “granular domain” in the initial stages of weathering and a “clay matrix domain” thereafter. As the compression mechanisms of a saprolitic soil can be expected to be different for these two domains and to span across the mechanical behaviours discussed above, it would be desirable to find a trend analogous to that of Baynes & Dearman, but based on mechanical parameters. However, this could only be an approximate trend as weathered soils are generally well graded and are seldom found in nature having a perfectly fractal or binary grading, which are idealisations often used in research to establish general frameworks.

In this work one-dimensional compression tests were carried out on granitic saprolitic soils with different weathering degrees. Isotropic and one-dimensional compression tests on other saprolites from Hong Kong and around the world were reanalysed and compared with those tested here to establish general trends.

### **Soils Tested**

The soils tested in this work were a saprolite from the Sha Tin Granite sampled along a slope profile and a saprolite from the Kowloon Granite, sampled at shallow depths. According to the GEO (1988) classification system, the soils tested belonged to grades IV to VI. In the Sha Tin Granite, several Mazier samples were taken in two boreholes, one covering depths between 6.5 and 27m (BHA), while the other only reached shallow depths (BHB). However, this would correspond to a depth of approximately 40m for the other borehole, due to the difference in ground level, which explains its being less weathered despite the shallower depth. Although it is expected that the weathering would generally be larger at the surface and decrease with depth, this was not rigorously observed. This type of non-uniformity is a typical feature of weathering and might be explained by preferential water

flow, such as along discontinuities. Two block samples were taken in the Kowloon Granite, both above 2m depth. The two samples were taken in two different trial pits (TPA and TPB), but were close together and belonged to the same geological formation. The acronyms used for the soils tested and their depths are reported in Table 1.

### **Gradings and Mineralogy**

To limit the heterogeneity of the dataset taken from the literature, only saprolitic soils originating from granites were taken into consideration. In Table 2 the details of the dataset available are listed. As mentioned above, the soils tested specifically for this research were from the Sha Tin Granite, where the soil was sampled at different depths with weathering degrees ranging from HDG to CDG, and the Kowloon Granite, which was sampled at shallower depths and included both CDG and RS. Besides these soils, a number of the other sets of data considered were from Hong Kong. In particular, the data from Fung (2001), Zhang (2011) and Madhusudhan & Baudet (2014) are also from the Kowloon Granite, while the data from Ng & Chiu (2003) and Yan & Li (2012) are from the Mt. Butler and the Needle Hill Granites, respectively. The other data considered are from Korea (Lee & Coop, 1995 and Ham et al., 2010), Portugal (Viana da Fonseca, 1998 and Viana da Fonseca et al., 2006) and Japan (Ham et al., 2010).

In Figure 1 the gradings of these soils are presented. The solid symbols refer to the soils tested in this work, while the open symbols are for the other saprolites from Hong Kong and the cross symbols for saprolites from other locations in the world. To have an easier, although coarser, means of comparison, the particle size distributions were divided into three parts, i.e. gravel, sand and fines, which are the sum of the silt and clay fractions. The grading curves of the soils tested for this work are presented in Figure 2 and the others can be found in the relevant references. In Viana da Fonseca (1998) a great number of grading curves was presented, and the limits of the envelope formed by these curves are shown as a hatch shaded

diamond area in Figure 1. The envelopes proposed by Lumb (1962) for the Highly Decomposed Granite, Completely Decomposed Granite and Residual Soil, which were based on a large dataset from Hong Kong, are superimposed on Figure 1 to provide a reference regarding the weathering degrees. In general, most of the soils analysed fall in or close to the envelopes proposed by Lumb, except for those soils plotting on the *finer* axis, for which a possible explanation will be given later in this section. As the weathering degrees of the soils outside Hong Kong were generally not specified, the agreement might be to some extent fortuitous. However, except for the Sha Tin Granite, where only one sample was identified as HDG on the borehole log but a few actually plot in that area, all the other data from the literature in Hong Kong were described as CDG and also plot in the CDG area.

The data on Figure 1 are quite scattered and this may result from the variability of grain size in the parent rock, although this will, to some extent, be bounded by the description that they are all granites and not rhyolites or pegmatites. Unfortunately most authors have not stated whether or not they have curtailed their gradings curves at the larger particle sizes for testing. In the tests conducted here, the gradings were curtailed at 6.3mm or 5mm and the effect that this has on the grading is indicated in Table 2 and Figure 1 as it is for Lee & Coop (1995) where this information is also available. Unfortunately it is not possible to know exactly the consequences of the curtailing on correlations between grading and mechanical behaviour, since both the grading descriptors and the compressibility are likely to change as a result. The “intact gradings” are presented in Figure 1 with grey symbols and on Figure 2 the intact and curtailed gradings curves for this research are compared in detail. Although only in one case (6) there was no curtailing and the amount of discarded particles for some of the other tests in this research might seem significant, the particles larger than 6.3mm might be more appropriately considered as “rock lumps”, since the maximum size of the mineral grains in the parent rocks was not larger than 2-5mm. Even so, gravel makes up the majority of the

grading curve in most cases. The soils tested by Ham et al. (2010) and Zhang (2011) were curtailed at a relatively small particle size of 2mm so they plot on the *finer* axis in Figure 1 and would explain their anomalous position with respect to the envelopes proposed by Lumb (1962). However, it is not known what proportion of coarser particles were discarded, although the low proportion of fines in Ham et al. (2010) is more typical of a less weathered soil and the resulting curtailment leaves the soil with a relatively unusual grading as a more poorly graded soil than the others, composed mostly of sand. As discussed later, this may have an impact on their behaviour that influences their agreement with the correlations investigated.

In Figure 3 the mineralogical compositions of the soils are presented, which in the present work were determined by means of XRD analysis carried out on bulk soil samples, which were dried at 50°C and milled to <60µm. These were not available for every soil analysed and, in addition, the data for the Mt. Butler and Kowloon Granites were taken from a different source to the gradings data (Irfan, 1996). The minerals were divided into three groups, similarly to the gradings: quartz, feldspars and others, which include both the micas retained from the parent rock and the products of the weathering, such as clay minerals. Although the data are still quite dispersed, the scatter is slightly less than for the gradings.

### **Testing Methodology**

In this research, the soils were tested in conventional oedometers having 50mm diameter rings. Since the maximum grain size was as large as 20mm, as already mentioned the grading curves were terminated at 6.3mm or in some cases 5mm, as shown in Figure 2, to ensure a ratio of at least 6 between the ring diameter and the largest size of particles, as suggested by Lacasse & Berre (1988) for well graded soils, while being able to achieve elevated stresses in a standard equipment. The reconstituted soil was mixed to the required proportions of each particle size having first separated the soil from each weathering degree



into the usual sieve intervals by dry sieving. All the soils considered from other work in the literature were tested in a reconstituted state but it is not known in detail what were the preparation processes adopted.

The parameters used as a reference in this study are the slope of the Normal Compression Line (NCL) in the volumetric plane ( $\lambda = \Delta v / \Delta \ln p'$  where  $v$  is specific volume and  $p'$  the mean normal effective stress) and the specific volume on the NCL at 100kPa ( $N_{100}$ ). As can be seen in Table 2, some of the  $\lambda$  values calculated were obtained from oedometer tests (1D), while others were from isotropic compression carried out in triaxial cells (ISO). When comparing the values obtained from oedometer and triaxial tests, it is therefore implicitly assumed that the isotropic and one-dimensional NCLs are parallel in the volumetric plane. This means that  $\lambda = C_c / 2.303$ , where  $C_c$  is the compression index defined in terms of  $\log_{10}$  vertical stress for an oedometer test, so that it is also assumed that  $K_0$  is constant on the NCL. However, since the  $K_0$  values were not available for all cases, the  $N_{100}$  was determined only for the oedometer tests. The value of the specific volume at 100kPa vertical stress ( $N_{100}$ ) was chosen, since  $\lambda$  was estimated approximately in the stress range 100-1000kPa. The more commonly used intercept at 1kPa would be badly affected by small changes in  $\lambda$ . The NCLs were chosen to be straight within the pressure ranges tested when interpreting the data and more importance was given to the tests that reached larger stress, therefore using the slope of the tests after yielding occurred to calculate  $\lambda$  as discussed below.

## **Results and Discussion**

### **Correlation between compressibility and grading descriptors**

Figures 4a to c show the one-dimensional compression tests carried out in this work. An explanation of the sample names is given in Table 1. For each soil a number of tests were carried out covering a wide range of initial specific volumes when preparing the reconstituted

samples. The samples were created either by gentle moist tamping, which was carried out by hand varying the water content from 8 to 60%, or by mixing to a slurry for the soils having a larger amount of fines. The range of initial specific volumes that could be achieved changed with the soil, due to the differences in their initial gradings, since more efficient packing modes are obtained as the mean particle size reduces and the grading curve becomes flatter. However, it is clear that after yielding each soil defines a unique NCL, which have been indicated in Figure 4. In some cases, only one loose specimen and one dense one were tested, but the NCL was nonetheless well defined. This is because exactly the same grading was used for all the specimens within each weathering degree, which corresponded to the average grading curve calculated for that soil from a much larger sample so that any minor heterogeneity would not cloud the trends further. The NCLs from the literature data were derived in the same way.

Rocchi et al. (2015) have shown that for a granitic saprolite the characteristic dominating the behaviour in compression is grading, rather than mineralogy or particle morphology. For this reason and because the mineralogy and particle morphology were not always available for the dataset analysed, the changes in the NCL slope and intercept were correlated with several grading descriptors that are more commonly used in engineering practice.

Among the parameters considered were the mean size  $D_{50}$ , the amount of fines, the coefficient of uniformity  $c_u$ , the coefficient of curvature, the fractal dimension (if appropriate) and the breakage potential  $B_p$ , (as defined by Hardin, 1985). However, all these parameters describe the initial grading curve with one value only, whereas two are really required, one describing the shape of the curve (well or poorly graded) and the other defining its location arising from the size of the particles. An attempt to define such a parameter for sedimentary soils was made by Cola & Simonini (2002), who proposed the grain size index  $I_{GS}$ . This is the

ratio of  $D_{50}$  and  $c_u$ , where the former is normalised by 1mm ( $D_0$ ) to make it dimensionless, i.e.  $I_{GS}=(D_{50}/D_0)/c_u$ . This parameter therefore includes both the location of a grading curve and its shape. However, it did not show any evident improvement in the trends observed when it was considered and so only the three most common parameters are presented here,  $D_{50}$ , % fines content and  $c_u$ .

In Figure 5 the results are analysed with respect to  $D_{50}$ . For a uniform granular material, a trend would be expected for soils with larger particles to be more compressible, as breakage increases with particle size (Weibull, 1951) and sands become more compressible. As the yield stress in compression reduces with increasing particle size, the intercept  $N_{100}$  would also be expected to increase with size (McDowell 2002). From a consideration of mixed binary soil gradings, as discussed above decreasing  $D_{50}$  would again be expected to cause a reduction of  $\lambda$  down to a minimum after which it might be expected to increase again. Examining only the data from this study (the solid symbols) in Figure 5a, a reasonably clear trend can be seen for  $\lambda$  to reduce with particle size down to a size below 1mm, while below this value  $\lambda$  may be less sensitive to changes in  $D_{50}$ . Most of the data from other sources plot reasonably close to this trend, especially for the other Hong Kong soils. With the exception of Viana da Fonseca et al. (2006), the data that present some scatter are mainly for soils where the maximum size has been curtailed significantly, notably the data of Ham et al. (2010), as this directly affects the  $D_{50}$  values, and may have an effect on  $\lambda$  too. Zhang & Baudet (2013) observed that  $D_{max}$  might be more significant for breakage, and therefore the compressibility of a mixture, than its amount of fines. With the sparsity of data at the finer sizes the trend identified is slightly tentative, but the two parts of the trend proposed might mark a change in the compression mode, and the reduction of  $\lambda$  with decreasing  $D_{50}$  is what is commonly seen for the binary soil mixtures typically used in research (e.g. Carrera et al., 2011). Within the

limited dataset it is not possible to see if the trend reaches a minimum and reverses direction as is observed for binary mixtures.

Given any pair of points 1 and 2 in Figure 5a, the null hypothesis ( $H_0$ ) was formulated so that  $D_{50}$  and  $\lambda$  are not correlated, i.e. if  $D_{50}(1) > D_{50}(2)$  then  $\lambda(1) > \lambda(2)$ ,  $\lambda(1) = \lambda(2)$  and  $\lambda(1) < \lambda(2)$  have the same probability to be true. Then the joint probability  $P(A | B) = 1/3$  considering A  $D_{50}(1) > D_{50}(2)$  and B  $\lambda(1) > \lambda(2)$  as independent events, i.e. no correlation between  $D_{50}$  and  $\lambda$ . For this null hypothesis  $p = 0.33$ , which is much larger than the significance level  $\alpha = 0.05$  usually set. However, carrying out a statistical analysis of the dataset assuming the alternative hypothesis ( $H_1$ ) “if  $D_{50}(1) > D_{50}(2)$  then  $\lambda(1) > \lambda(2)$  or else if  $D_{50}(1) < D_{50}(2)$  then  $\lambda(1) < \lambda(2)$ ”, this was true for 60% of the sample, which is much larger than the probability of  $H_0$ . When excluding the data for those soils whose gradings were curtailed at 2mm, the probability improved to about 66%.

Due to the several parameters that should influence  $\lambda$ , it is unlikely that any simple relationship like that in Figure 5 will completely describe the phenomenon, and the formulation of a complete model would be highly complex, perhaps including not only the location of the gradings curve but details of its shape, the particle morphologies, mineralogies and strengths as well as the parent rock crystal size. Unravelling the effects of all these possible factors would require an extremely large dataset that does not currently exist, nor is likely ever to, and so it is still useful to identify the effect that simple indices such as  $D_{50}$  have, even if the relationships derived are inevitably scattered. The agreement of the trends with what would be expected from the literature for other, simpler soils helps improve confidence in them. Any cause of systematic error that adds to the scatter, such as  $D_{max}$ , is difficult to identify due to the reduced dataset.

The trend for  $N_{100}$  in Figure 5b is quite similar to that for  $\lambda$ , with slightly less scatter. It is possible that this is due to some extent because only oedometer tests were considered. The reducing value of intercept with decreasing  $D_{50}$  is again typical of what is seen in the literature for binary soil mixtures (e.g. Carrera et al., 2011) but the data do not indicate whether at even finer gradings the intercepts would start to increase again as is commonly observed.

In Figure 6, the data are presented with respect to the amount of fines, since in binary mixtures this is used as an indicative parameter to predict the type of behaviour, i.e. granular, intermediate or fines dominated. Although the data for gradings curtailed at a smaller size agree better with the trend proposed than in Figure 5, the data scatter is overall much greater as showed by the 30% value of probability, calculated similarly than for  $D_{50}$ . The labels adjacent to the data points indicate the plasticity index where known. A consistent trend compared to that seen in Figure 5 can be observed, with  $\lambda$  reducing as fines content increases, but again no evidence of a minimum within the range of data could be found. Although there is only one data point for a large amounts of fines, its value is similar to the average for the points at around 30-40% fines, which might suggest an approximately constant trend. This could be because the plasticity index has similar values for these soils, with the exception of only one data point for the Kowloon Granite, which plots well outside the trend. The variability of the  $\lambda$  values in the granular matrix domain, i.e. values below 10% of fines, is then strikingly more than that observed in the fines matrix domain, where the clay mineralogy might be more important. This is probably because the dataset chosen was carefully selected to include only granitic saprolites, which are then more likely to result in similar mineralogical compositions with weathering. The conclusions drawn by Rocchi et al. (2015), i.e. that grading and not mineralogy dominates the compressibility, seems therefore to

be confirmed based on the dataset analysed here. Similarly to the considerations made for  $D_{50}$ ,  $N_{100}$  is expected to reduce with increasing % of fines, which is observed in Figure 6b.

In Figure 7 the results are analysed with respect to  $c_u$ . In a granular soil, it is expected that soils with uniform gradings would compress more because of fewer points of contact among the particles (lower coordination numbers) resulting in higher forces acting across the contacts, a trend which can possibly be seen in Figure 7. However, an approximately linear trend is observed for both  $\lambda$  and  $N_{100}$ , with no break or change that is visible within the scatter that might indicate the two different domains. In one case  $c_u$  was defined as  $D_{70}/D_{20}$  due to difficulty in establishing  $D_{10}$  from the grading curve. However, this does make this value of  $c_u$  less reliable and it is identified with \* on the figure. Although the scatter of data seems to be noticeably worse on this plot than those either for  $D_{50}$  or fines content, the hypothesis that the higher the  $c_u$  value, the larger  $\lambda$  gave a probability of 72%. The soils having a curtailed  $D_{max}$  have been included and agree with the trend, when these are excluded the trend is actually worse and  $p=0.35$ . This could be because  $c_u$  describes the shape of the grading curve and not its position and so it is not so badly affected by a change to  $D_{max}$ . Once again the trend for  $N_{100}$  is less scattered than for  $\lambda$ , possibly because only oedometer tests have been included.

### **Breakage**

To shed light on the mechanisms of compression, the particle breakage was analysed in detail. The breakage was studied quantitatively in terms of relative breakage ( $B_r$ ), as defined by Hardin (1985), and in terms of changes of shape using a Qicpic laser scanner (Sympatec, 2008). The parameters used for describing the shape of the particles were the aspect ratio (AR) and the convexity (C), which Zhang & Baudet (2015) suggested to be the most appropriate shape descriptors to indicate catastrophic particle breakage as opposed to chipping of the asperities. The aspect ratio is defined as the ratio of the minimum Feret

diameter to the maximum one, where the Feret diameter is the distance between any pair of parallel lines that touch two points on the particle perimeter without cutting through the particle silhouette (i.e. between apexes on the perimeter). The convexity is the ratio between the area of the particle silhouette and its convex hull, which is defined as that area which would be enclosed by an elastic rubber band if it were to be stretched around the particle silhouette (i.e. an area that includes all re-entrant parts of the silhouette).

Hardin (1985) defined  $B_r$  as the ratio of total breakage,  $B_t$ , which is the area between the gradings curves before and after testing, considering only that part above  $74\mu\text{m}$ , and the breakage potential,  $B_p$ , which is the area between the initial gradings curve and a cut-off at  $74\mu\text{m}$ . Coop & Lee (1993) showed that the sand particles begin to undergo significant breakage when reaching the NCL and thereafter a logarithmic trend between  $B_r$  and the mean effective stress could be observed. Even if many of the tests reached the same maximum stress, a similar trend can still be observed in Figure 8. However, Altuhafi & Coop (2011) showed that the amount of breakage measured not only depends on the stress reached, but also on the initial specific volume. Particles in a loose state have fewer points of contact between each other and therefore experience larger stresses. For this reason, only tests having a value of specific volume between 1.9 and 2.1 are presented at the highest stress level to limit the data scatter. For the other tests, the  $v_0$  is indicated in the label. The dp and sh ewCDG seem to plot slightly lower than the evwCDG and possibly the HDG, therefore suggesting that the breakage is less for the more weathered soils. This result might seem counterintuitive, but it arises from the better graded nature of the more weathered soils. Although it might seem that the breakage changes for different weathering degrees, when taking only the tests at the highest stress level, which represent the majority, and comparing them with their initial specific volumes, no real difference between the different degrees of weathering can be observed (Figure 9).

In Figure 9 it is evident that despite the different particle size distributions of each soil, the breakage undergone is very similar, and the trends only differ at high values of the initial specific volume, where some scatter can be observed in the data, but without any clear effect of degree of weathering. This contrasts with Ham et al. (2010) who emphasised the effect of weathering degree on the strength of grains of granitic saprolites. However, their conclusions were mainly based on single particle crushing tests, while they did not calculate a global breakage for the different weathering degrees. As already mentioned, Zhang & Baudet (2013) observed that  $D_{\max}$  seems to dominate breakage rather than the amount of fines in a mixture, which might explain the similarity of the data, since  $D_{\max}$  changes little with weathering (Figure 2). Although it might be regarded as just another gradings descriptor like  $c_u$  or  $D_{50}$ , Hardin intended that the value of  $B_p$  should represent the propensity of a soil to undergo particle breakage. When comparing the  $\lambda$  values with the corresponding  $B_p$  values (Figure 10), there is indeed a clear trend for the soils tested in this work (solid symbols), even if the  $B_r$  values were actually similar. This trend is not as evident for the soils from the literature, but  $B_r$  values were not available for many of them to examine how much breakage they underwent.

In Figure 11 the breakage is analysed for each grading component in a differential way. For this purpose, the difference in the cumulative mass before and after the test, defined as  $\Delta$  in the inset of Figure 11a, was calculated for the different grain sizes. For the stress level reached of 7MPa, there is a net gain in mass for each size component except for the maximum. This of course does not mean that there is no breakage for components of the gradings curve where there is a net gain, as can be seen if the difference in passing mass is calculated ( $\delta$  in Figure 11b). When comparing the cumulative curves,  $\Delta$  is greatest at 2mm size, where a peak is visible for all soils except the sh ewCDG. This peak corresponds to the change between negative and positive values in  $\delta$ , in Figure 11b. It is possible that the



particles larger than 2mm experience the largest change simply because they represent the majority of the retained soil in the grading curves for these soils. In Figure 11b, however, it can be seen that the highest net gain is for the grain size 0.3-0.6mm. Nakata et al. (1999) showed that catastrophic splitting is essentially of two types, according to the strength of the mineral. Strong minerals have a single and well defined peak strength and particle breakage typically results in two large pieces being left after breakage, while weaker minerals like feldspars suffer progressive breakage of the particle asperities resulting in numerous grain pieces and multiple peaks in its strength. Although in this research the particles of the soils tested consisted of aggregates of different minerals, it would appear that the main mechanism of breakage is progressive failure of the particles as the greatest loss is at the 2-5mm size, while the maximum net gain is at 0.3-0.6mm.

In Figure 12 the shape descriptors described above were analysed for the particles retained in the sieves immediately below and above 2mm, before and after testing. The comparison could also be carried out using all the particles that are below or above 2mm. However, the maximum size that can be analysed by the Qicpic apparatus is 4mm and the resolution of the descriptors depends on the ratio between particle and pixel size, i.e. the greater the better. In both Figures 12a and b, it can be observed that the change of shape is significantly larger for particles greater than 2mm. These changes of shape reduce progressively to zero with reducing particle size, as shown in the insert in Figure 12a. It would therefore appear that particles larger than 2mm experience catastrophic splitting, while the remainder of the grading is less affected by breakage and probably changes morphology more as a consequence of particle chipping and abrasion.

The sh ewCDG presents a different mode of breakage in Figure 11, as there is no clear peak at 2mm or any other grain size. The values of  $\Delta$  and  $\delta$  describe a flatter curve which has lower values than the others. Figure 13 shows the values of aspect ratio below and

above 1mm, where a slight change in slope can be observed in Figure 11. A significant change in the shape distribution before and after testing is seen in both cases. This might indicate that breakage is experienced similarly across the whole particle size distribution. However, further research is needed to investigate how breakage evolves for soils having greater amounts of fines and to explain how different breakage modes can result in similar overall values of  $B_r$ .

## Conclusions

The compression of reconstituted samples of weathered granitic saprolites were studied based on a number of tests carried out on a range of weathering degrees and analysing the existing literature. A trend of reducing compressibility with reducing  $D_{50}$  was found, as might be expected either from considerations of grading change or particle breakage. It appeared that while there was a clear reduction of compressibility in the granular matrix domain identified by Bayne & Dearman (1978), there was no clear change in the fines matrix domain. In contrast a monotonic linear trend was found with increasing  $c_u$ , although more scatter was observed in this case, perhaps indicating the inability of  $c_u$  to distinguish the domains. The maximum size appears to be also an important factor when analysing the behaviour with respect to the grain size.

When analysing the breakage in an attempt to illustrate the mechanisms of compression, it was found that the relative breakage undergone by the soils tested was rather similar, despite the differences in their grading curves and degrees of weathering. When studying breakage in more detail, it was observed that the larger particle sizes, which also represented the majority of the soil by mass before testing, experienced the most breakage. In addition, comparing the particle morphology of the different grain sizes before and after testing, it was observed that these particles experienced catastrophic breakage, while the smaller grains probably changed as a result of smaller scale particle damage such as chipping.

### List of symbols and abbreviations

AR	aspect ratio
$B_p$	breakage potential
$B_r$	relative breakage
$B_t$	total breakage
C	convexity
$C_c$	compression index
$c_u$	coefficient of uniformity
$D_0$	reference size, 1mm
$D_{10}, D_{20}, \text{etc.}$	particle diameters at 10%, 20%, etc. of passing mass of soil
$D_{50(1)}, D_{50(2)}$	mean particle diameter for soil No.1 and No.2.
$D_{\max}$	maximum grain size
$H_0$	null hypothesis
$I_{GS}$	Grain size index $(D_{50}/D_0)/c_u$
$K_0$	coefficient of earth pressure at rest
$N_{100}$	value on the NCL at $\sigma'_v=100\text{kPa}$
NCL	Normal Compression Line

$p$	the probability of observing an effect given that the null hypothesis is true
$v$	specific volume
$v_0$	initial specific volume
$\alpha$	significance level
$\delta$	difference between the percentage retained at a given particle size before and after testing
$\Delta$	difference between the cumulative percentage retained at a given particle size before and after testing
$\lambda$	gradient of the NCL or 1D-NCL
$\lambda(1), \lambda(2)$	$\lambda$ for soil No.1 and No.2.
$\sigma'_v$	vertical stress in the oedometer test

### **Acknowledgments**

The work described in this paper was fully supported by a grant from the Research Grants Council of the Hong Kong Special Administrative Region, China (Project No. CityU 112911). The authors would like to express their gratitude to Dr. John Endicott from AECOM and Ir Ken Ho from GEO for kindly providing the samples tested. The authors would also like to express their gratitude to Prof. Charles Ng and Prof. Quentin Yue for permission to use their data and to Dr Béatrice Baudet of the University of Hong Kong for the use of the Qicpic particle laser scanner.

## References

- Altuhafi F & Coop MR (2011) Changes to particle characteristics associated with the compression of sands. *Géotechnique* 61(6): 459-471.
- Baynes FJ & Dearman WR (1978) The relationship between the microfabric and the engineering properties of weathered granite. *Bulletin of the International Association of Engineering Geology* 18(1):191-197.
- Carrera A, Coop MR & Lancellotta R (2011) Influence of grading on the mechanical behaviour of Stava tailings. *Géotechnique* 61(11):935-946.
- Cola S & Simonini P (2002) Mechanical behavior of silty soils of the Venice lagoon as a function of their grading characteristics. *Canadian Geotechnical Journal* 39(4):879-893.
- Coop MR & Lee IK (1993) The behaviour of granular soils at elevated stresses. *Predictive Soil Mechanics, Wroth Memorial Symposium, Thomas Telford, London:186–198.*
- Coop MR, Sorensen KK, Bodas Freitas T & Georgoutsos G (2004) Particle breakage during shearing of a carbonate sand. *Géotechnique* 54(3):157-163.
- Fung WT (2001) Experimental study and centrifuge modelling loose fill slope. M.Phil., Hong Kong University of Science and Technology, Hong Kong.
- Geotechnical Engineering Office (1988) Guide to rock and soil descriptions. *Geoguide 3*. Geotechnical Engineering Office, Hong Kong.
- Ham TG, Nakata Y, Orense R & Hyodo M (2010) Influence of water on the compression behavior of decomposed granite soil. *ASCE Journal of Geotechnical and Geoenvironmental Engineering* 136(5):697-705.

- Hardin BO (1985) Crushing of soil particles. *ASCE Journal of Geotechnical and Geoenvironmental Engineering* 111(10):1177-1192.
- Irfan TY (1996). Mineralogy and fabric characterization and classification of weathered granitic rocks in Hong Kong. Geotechnical Engineering Office Report no.41, Geotechnical Engineering Office, Hong Kong.
- Lacasse S & Berre T (1988) Triaxial testing methods for soils. *Advanced Triaxial Testing of Soil and Rock*, ASTM STP 977. eds Donaghe RT, Chaney RC and Silver ML, American Society for Testing and Materials, Philadelphia:264-289.
- Lade JA & Yamamuro PV (1997) Static liquefaction of very loose sands. *Canadian Geotechnical Journal* 34(6):905-917.
- Lee IK & Coop MR (1995) The intrinsic behaviour of a decomposed granite soil. *Géotechnique* 45(1):117-130.
- Lumb P (1962) The properties of decomposed granite. *Géotechnique* 12(3):226-243.
- Madhusudhan BN & Baudet BA (2014). Influence of reconstitution method on the behaviour of completely decomposed granite. *Géotechnique* 64(7):540-550.
- McDowell GR (2002) On the yielding and plastic compression of sand. *Soils and Foundations* 42(1):139-145.
- Miao G & Airey D (2013) Breakage and ultimate states for a carbonate sand. *Géotechnique* 63(14):1221-1229.
- Minh NH & Cheng YP (2013) A DEM investigation of the effect of particle-size distribution on one-dimensional compression. *Géotechnique* 63(1):44-53.

- Nakata Y, Hyde AFL, Hyodo M & Murata H (1999). A probabilistic approach to sand particle crushing in the triaxial test. *Géotechnique* 49(5):567-583.
- Ng CWW & Chiu ACF (2003) Laboratory study of loose saturated and unsaturated decomposed granitic soil. *ASCE Journal of Geotechnical and Geoenvironmental Engineering* 129(6):550-559.
- Rocchi I, Todisco MC & Coop MR (2015) Influence of grading and mineralogy on the behaviour of saprolites IS Buenos Aires 2015. Provisionally accepted.
- Sympatec (2008) Windox-operating instructions release 5.4.1.0. Sympatec, Clausthal-Zellerfeld, Germany.
- Thevanayagam S & Mohan S (2000). Intergranular state variables and stress-strain behaviour of silty sands. *Géotechnique* 50(1):1–23.
- Thevanayagam S, Shentham T, Mohan S & Liang J (2002) Undrained fragility of clean sands, silty sands and sandy silts. *ASCE Journal of Geotechnical & Geoenvironmental Engineering* 128(10):849-859.
- Viana da Fonseca A (1998) Identifying the reserve of strength and stiffness characteristics due to cemented structure of a saprolitic soil from granite. *The geotechnics of hard soils – soft rocks: Proceedings of the 2<sup>nd</sup> International Symposium on Hard Soils – Soft Rocks*. Balkema, Rotterdam:361-372.
- Viana da Fonseca A, Carvalho J, Ferreira C, Santos JA, Almeida F, Pereira E, Feliciano J, Grade J & Oliveira A (2006) Characterization of a profile of residual soil from granite combining geological, geophysical and mechanical testing techniques. *Geotechnical and Geological Engineering* 24:1307-1348.

- Weibull B (1951) A Statistical Distribution Function of Wide Applicability. *Journal of Applied Mechanics* 18:293-297.
- Yan WM & Li XS (2012) Mechanical response of a medium-fine-grained decomposed granite in Hong Kong. *Engineering Geology* 129-130:1-8.
- Zhang J (2011). Laboratory investigation of loosely compacted completely decomposed granite for slope design. M.Phil., University of Hong Kong, Hong Kong.
- Zhang X & Baudet BA (2013) Particle breakage in gap-graded soils. *Géotechnique Letters* 3(2):72–77.
- Zuo L & Baudet BA (2015) Determination of the transitional fines content of sand-non plastic fines mixtures. *Soils & Foundations* 55(1):213-219.

### List of tables

**Table 1** Depths of the samples tested and the acronyms used (BH borehole, TP trial pit)

**Table 2** Details of the soils used as a dataset. Note: values for intact gradings in brackets, n.d. not determined, 1D one-dimensional compression, ISO isotropic compression

### List of figures

**Fig.1** Gradings of granitic saprolites from several locations worldwide, superimposed with the change in grading hypothesised by Irfan (1996). <sup>1</sup> Lee & Coop (1995), <sup>2</sup> Viana da Fonseca (1998), <sup>3</sup> Fung (2001), <sup>4</sup> Ng & Chiu (2003), <sup>5</sup> Viana da Fonseca et al. (2006), <sup>6</sup> Ham et al. (2010), <sup>7</sup> Zhang (2011), <sup>8</sup> Yan & Li (2012) and <sup>9</sup> Madhusudhan & Baudet (2014)

**Fig.2** Particle size distribution of the soils tested for this research.



**Fig.3** Mineralogy of granitic saprolites from several locations worldwide. <sup>1</sup> Lee & Coop (1995), <sup>2</sup> Irfan (1996) and <sup>3</sup> Ham et al. (2010)

**Fig.4** One-dimensional compression tests and NCLs (a) sh ewCDG and evwCDG of the Sha Tin Granite, (b) dp ewCDG and HDG of the Sha Tin Granite and (c) ewCDG and RS of the Kowloon Granite

**Fig.5** Trends with mean size: (a) NCL slope and (b) NCL intercept. <sup>1</sup> Lee & Coop (1995), <sup>2</sup> Viana da Fonseca (1998), <sup>3</sup> Fung (2001), <sup>4</sup> Ng & Chiu (2003), <sup>5</sup> Viana da Fonseca et al. (2006), <sup>6</sup> Ham et al. (2010), <sup>7</sup> Zhang (2011), <sup>8</sup> Yan & Li (2012) and <sup>9</sup> Madhusudhan & Baudet (2014).

**Fig.6** Trends with % fines: (a) NCL slope and (b) NCL intercept. <sup>1</sup> Lee & Coop (1995), <sup>2</sup> Viana da Fonseca (1998), <sup>3</sup> Fung (2001), <sup>4</sup> Ng & Chiu (2003), <sup>5</sup> Viana da Fonseca et al. (2006), <sup>6</sup> Ham et al. (2010), <sup>7</sup> Zhang (2011), <sup>8</sup> Yan & Li (2012) and <sup>9</sup> Madhusudhan & Baudet (2014)

**Fig.7** Trend of compressibility with coefficient of uniformity: (a) NCL slope and (b) NCL intercept. <sup>1</sup> Lee & Coop (1995), <sup>2</sup> Viana da Fonseca (1998), <sup>3</sup> Fung (2001), <sup>4</sup> Ng & Chiu (2003), <sup>5</sup> Viana da Fonseca et al. (2006), <sup>6</sup> Ham et al. (2010), <sup>7</sup> Zhang (2011), <sup>8</sup> Yan & Li (2012) and <sup>9</sup> Madhusudhan & Baudet (2014)

**Fig.8** Particle breakage for the soils studied in this research. Trend with vertical stress

**Fig.9** Particle breakage for the soils studied in this research. Trend with specific volume

**Fig.10** Trend of compressibility with breakage potential. <sup>1</sup> Lee & Coop (1995), <sup>2</sup> Viana da Fonseca (1998), <sup>3</sup> Fung (2001), <sup>4</sup> Ng & Chiu (2003), <sup>5</sup> Viana da Fonseca et al. (2006), <sup>6</sup> Ham et al. (2010), <sup>7</sup> Zhang (2011), <sup>8</sup> Yan & Li (2012) and <sup>9</sup> Madhusudhan & Baudet (2014)

**Fig.11** Change in the grading components as a result of breakage: (a) cumulative curves and (b) histograms

**Fig.12** Change in the particle morphology as a result of breakage: (a) aspect ratio and (b) convexity

**Fig.13** Change in the particle morphology as a result of breakage for the sh ewCDG.

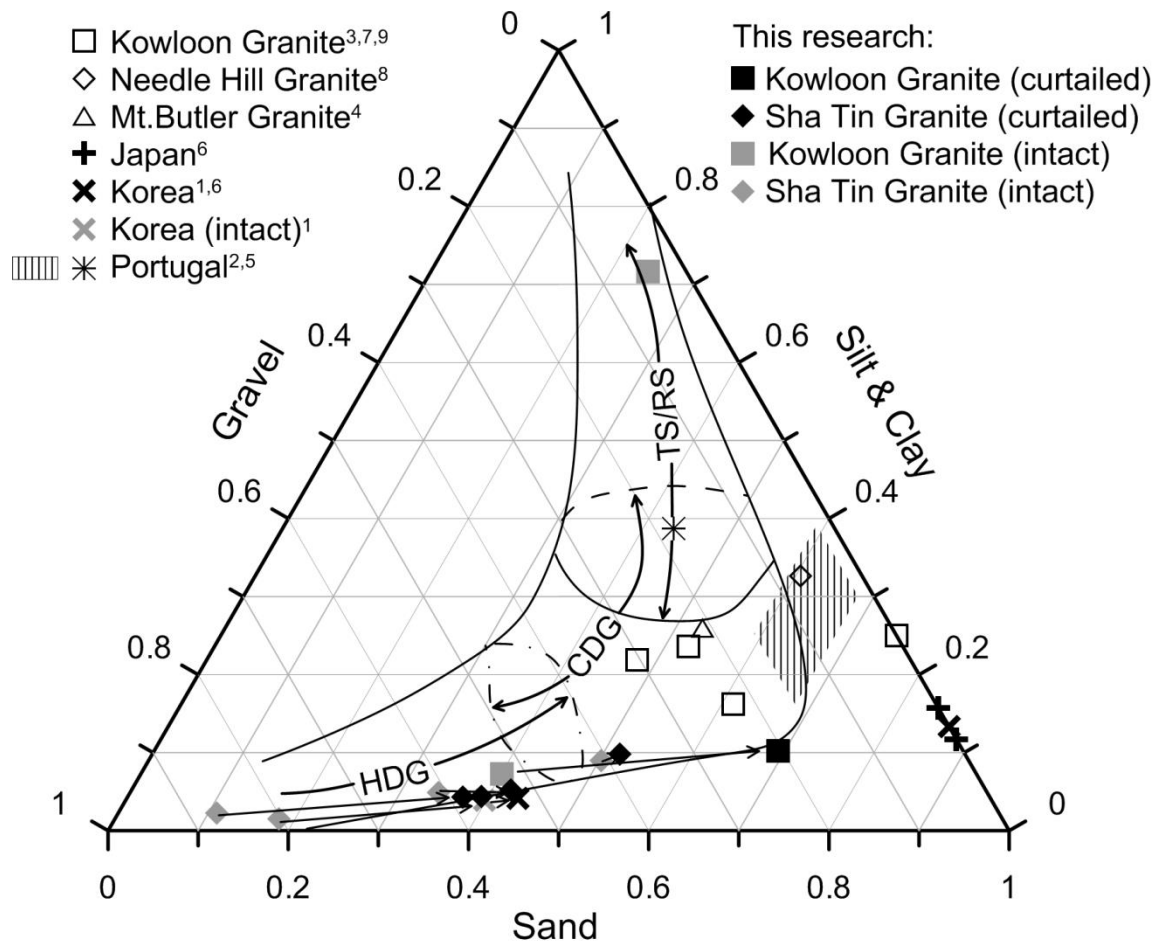
Soil description	Formation	Acronym	Depth (m b.g.l.)
extremely weak CDG	Sha Tin Granite	sh ewCDG	6.5-12 (BHA)
extremely to very weak CDG	Sha Tin Granite	evwCDG	12-20.5 (BHA)
extremely weak CDG	Sha Tin Granite	dp ewCDG	20.5-24 (BHA)
HDG	Sha Tin Granite	HDG	24-27 (BHA) and 5.8-6.3 (BHB)
extremely weak CDG	Kowloon Granite	ew CDG	1.4-1.7 (TPA)
RS	Kowloon Granite	RS	1.2-1.5 (TPB)

**Table 1** Depths of the samples tested and the acronyms used (BH borehole, TP trial pit)

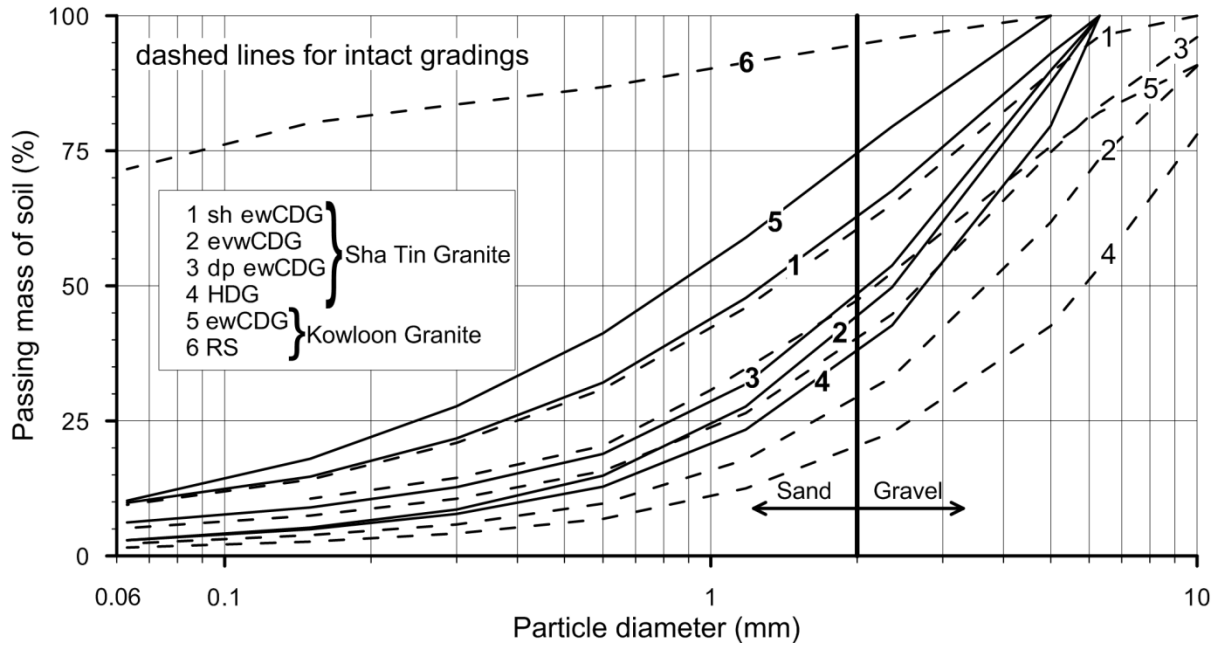
Source	Country	Formation	$D_{max}$ mm	$D_{50}$ mm	$c_u$	% fines	LL/ PL	$\lambda$	Test type
sh ewCDG (this work)	Hong Kong	Sha Tin Granite	6.3 (10)	1.36 (2.61)	32 (28)	10 (9)	n.d.	0.102	1D
evwCDG (this work)	Hong Kong	Sha Tin Granite	6.3 (20)	2.43 (3.92)	10 (8)	4 (2)	n.d.	0.15	1D
dp ewCDG (this work)	Hong Kong	Sha Tin Granite	6.3 (20)	2.07 (2.82)	10 (14)	4 (5)	n.d.	0.152	1D
HDG (this work)	Hong Kong	Sha Tin Granite	6.3 (20)	2.17 (5.85)	11 (8)	5 (1)	n.d.	0.139	1D
ewCDG (this work)	Hong Kong	Kowloon Granite	5 (20)	0.84 (2.18)	21 (23)	10 (7)	n.d.	0.088	1D
RS (this work)	Hong Kong	Kowloon Granite	5 (-)	0.01 (-)	157 (-)	72 (-)	n.d.	0.079	1D
Lee & Coop (1995)	Korea	-	6.3 (20)	2.13 (2.35)	12 (-)	4 (-)	n.d.	0.087	ISO
Viana da Fonseca (1998)	Portugal	-	5	0.14- 0.70	42- 89	16- 39	40/27	0.065	1D
Fung (2001)	Hong Kong	Kowloon Granite	5	0.88	563	22	44/26	0.068	ISO
Fung (2001)	Hong Kong	Kowloon Granite	5	0.71	113	24	79/41	0.132	ISO

Ng & Chiu (2003)	Hong Kong	Mt. Butler Granite	5	0.86	254	26	n.d.	0.128	ISO
Viana da Fonseca et al. (2006)	Portugal	-	10	0.13	43	39	n.d.	0.119	1D
Ham et al. (2010)	Japan	-	2	0.51	30	16	n.d.	0.142	1D
Ham et al. (2010)	Japan	-	2	0.60	15	12	n.d.	0.135	1D
Ham et al. (2010)	Korea	-	2	0.39	19	13	n.d.	0.143	1D
Zhang (2011)	Hong Kong	Kowloon Granite	2	0.56	283	25	n.d.	0.082	1D
Yan & Li (2012)	Hong Kong	Needle Hill Granite	5	0.30	214	33	38/23	0.091	ISO
Madhusudhan & Baudet (2014)	Hong Kong	Kowloon Granite	20	1.00	83	16	33/16	0.092	1D

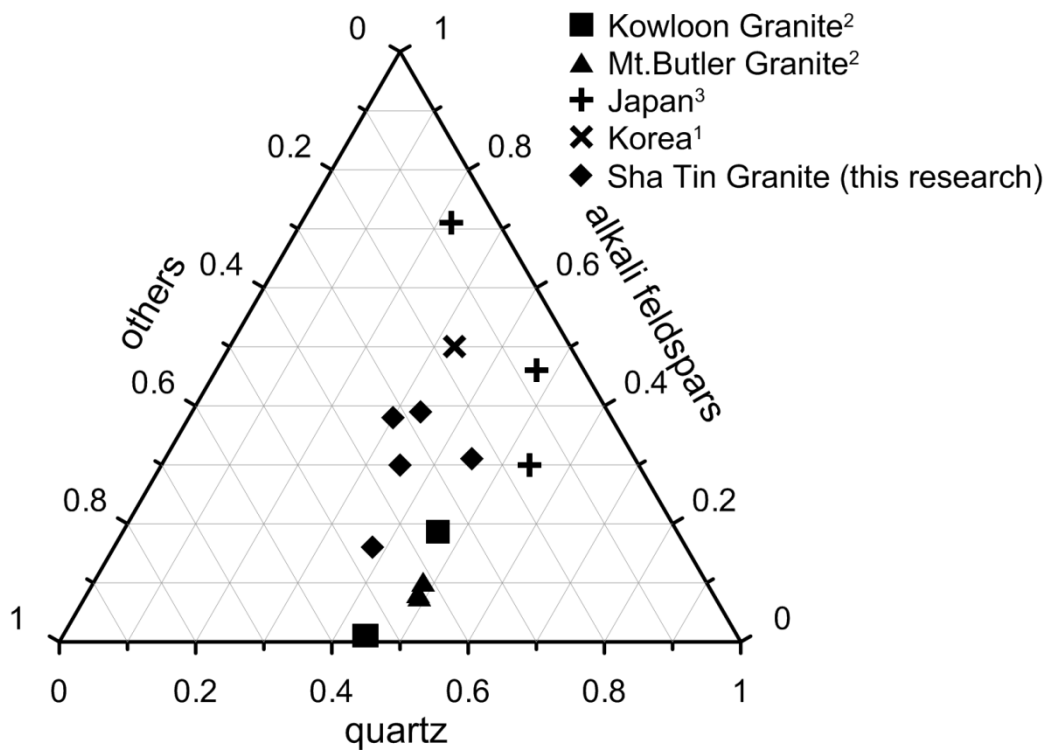
**Table 2** Details of the soils used as a dataset. Note: values for intact gradings in brackets, n.d. not determined, 1D one-dimensional compression, ISO isotropic compression



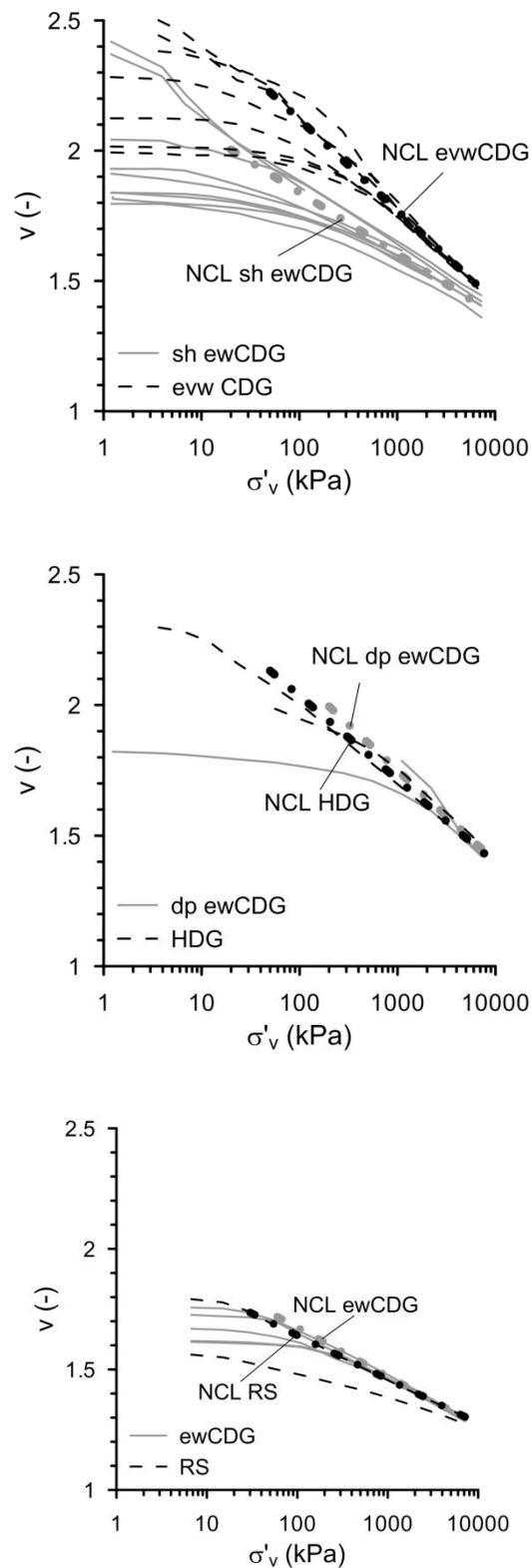
**Fig.1** Gradings of granitic saprolites from several locations worldwide, superimposed with the change in grading hypothesised by Irfan (1996). <sup>1</sup> Lee & Coop (1995), <sup>2</sup> Viana da Fonseca (1998), <sup>3</sup> Fung (2001), <sup>4</sup> Ng & Chiu (2003), <sup>5</sup> Viana da Fonseca et al. (2006), <sup>6</sup> Ham et al. (2010), <sup>7</sup> Zhang (2011), <sup>8</sup> Yan & Li (2012) and <sup>9</sup> Madhusudhan & Baudet (2014)



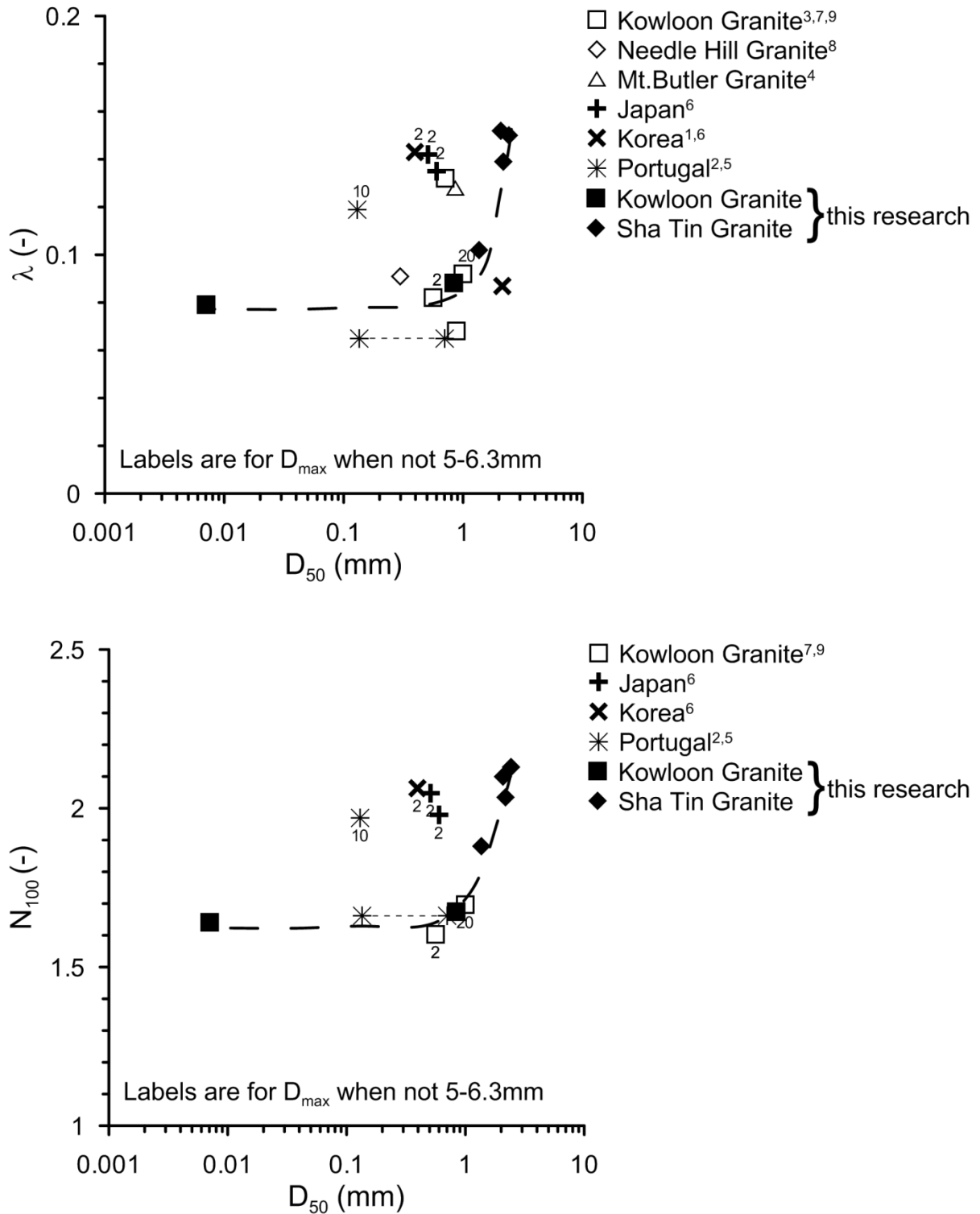
**Fig.2** Particle size distribution of the soils tested for this research.



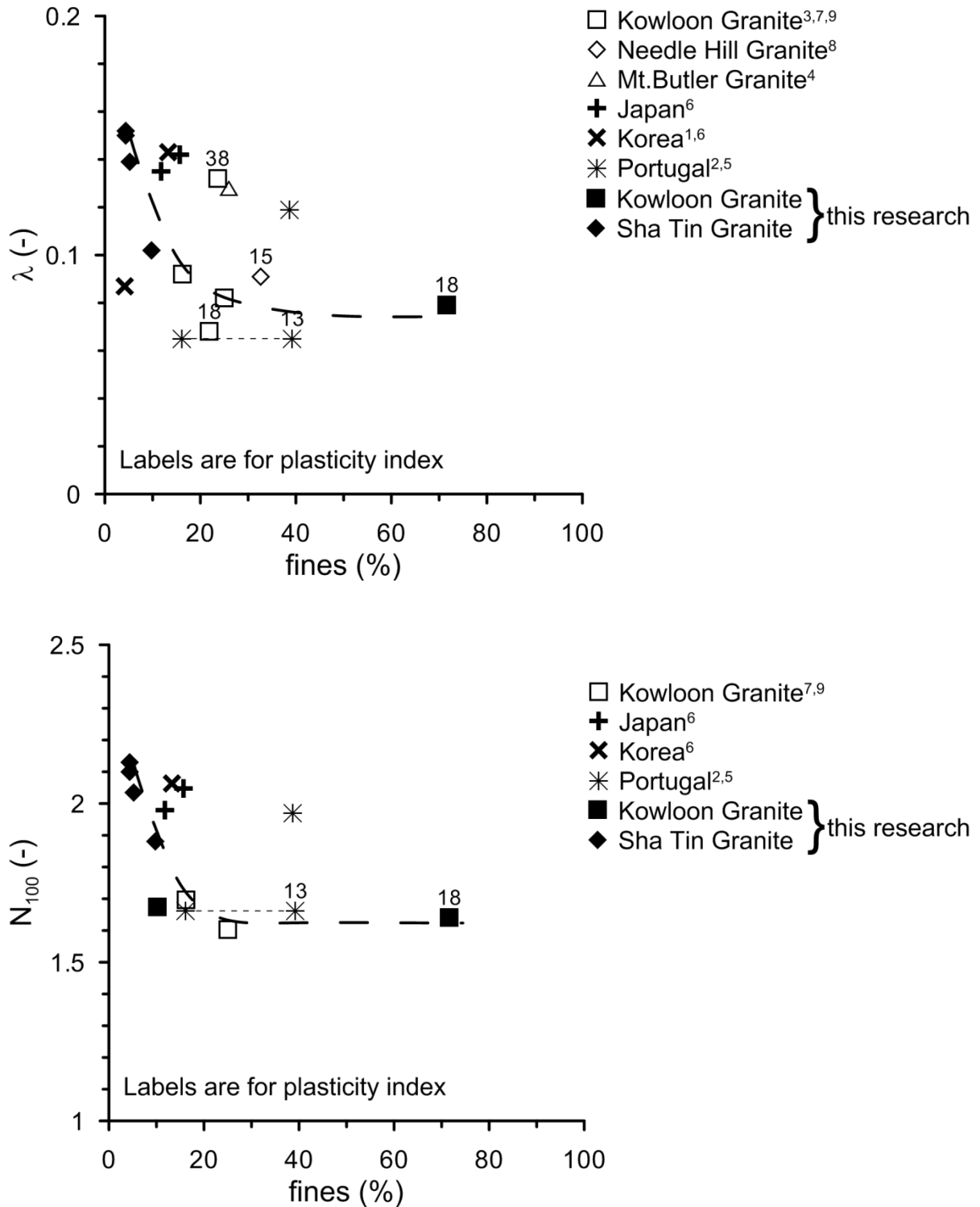
**Fig.3** Mineralogy of granitic saprolites from several locations worldwide. <sup>1</sup> Lee & Coop (1995), <sup>2</sup> Irfan (1996) and <sup>3</sup> Ham et al. (2010)



**Fig.4** One-dimensional compression tests and NCLs (a)  $sh\ ewCDG$  and  $ewwCDG$  of the Sha Tin Granite, (b)  $dp\ ewCDG$  and  $HDG$  of the Sha Tin Granite and (c)  $ewCDG$  and  $RS$  of the Kowloon Granite

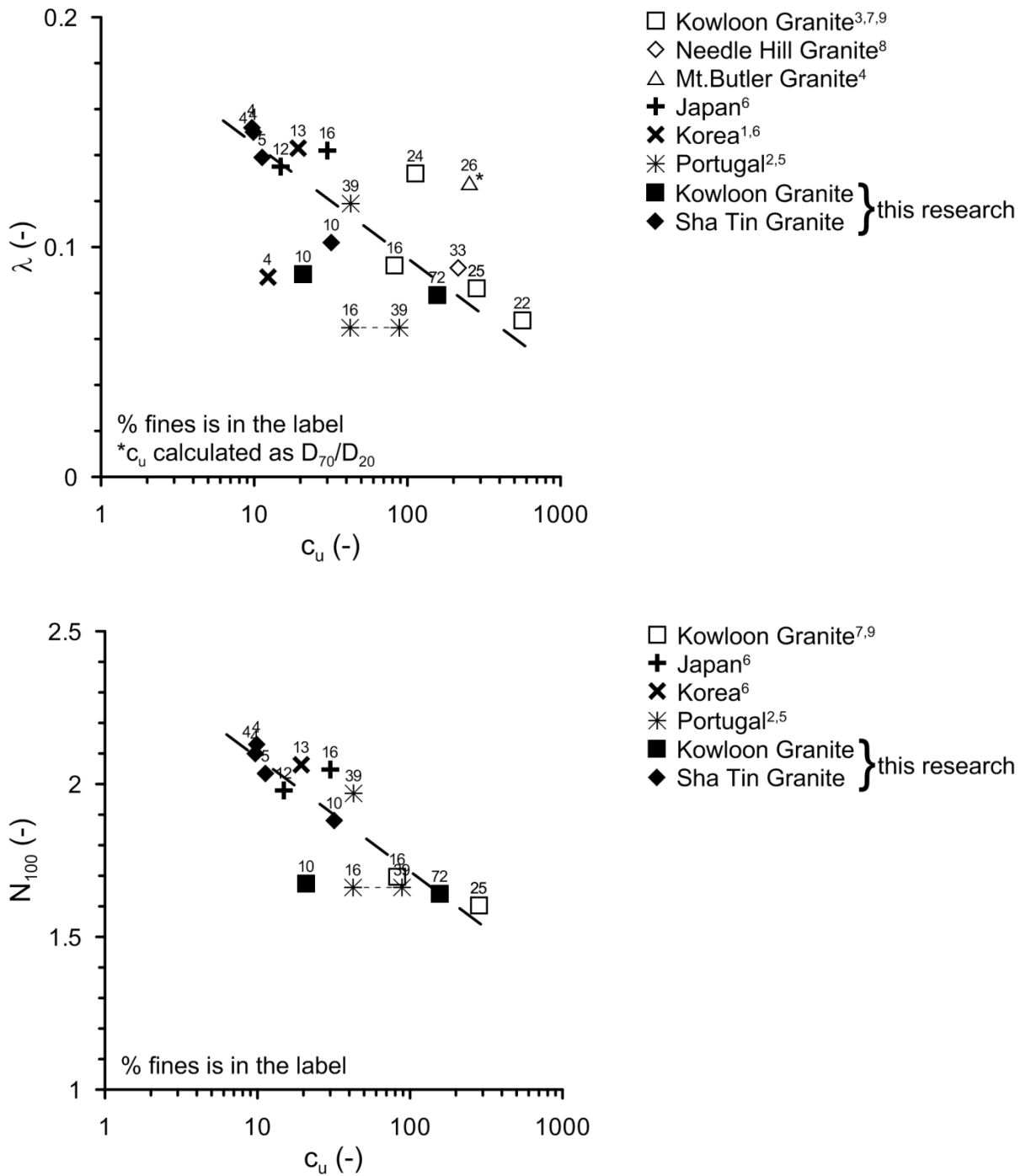


**Fig.5** Trends with mean size: (a) NCL slope and (b) NCL intercept. <sup>1</sup> Lee & Coop (1995), <sup>2</sup> Viana da Fonseca (1998), <sup>3</sup> Fung (2001), <sup>4</sup> Ng & Chiu (2003), <sup>5</sup> Viana da Fonseca et al. (2006), <sup>6</sup> Ham et al. (2010), <sup>7</sup> Zhang (2011), <sup>8</sup> Yan & Li (2012) and <sup>9</sup> Madhusudhan & Baudet (2014).

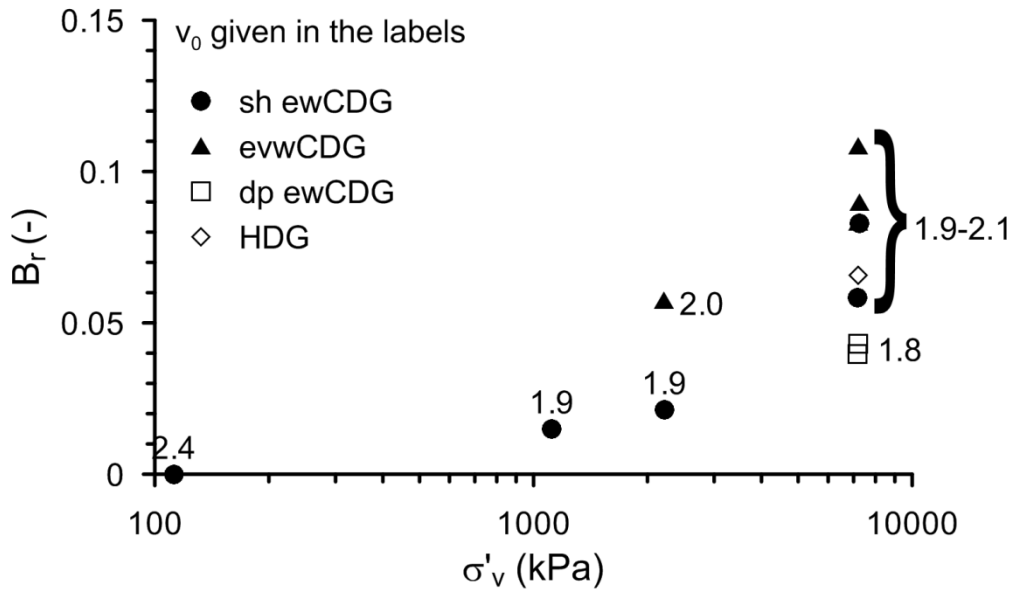


**Fig.6** Trends with % fines: (a) NCL slope and (b) NCL intercept. <sup>1</sup> Lee & Coop (1995), <sup>2</sup> Viana da Fonseca (1998), <sup>3</sup> Fung (2001), <sup>4</sup> Ng & Chiu (2003), <sup>5</sup> Viana da Fonseca et al. (2006), <sup>6</sup> Ham et al. (2010), <sup>7</sup> Zhang (2011), <sup>8</sup> Yan & Li (2012) and <sup>9</sup> Madhusudhan & Baudet (2014)

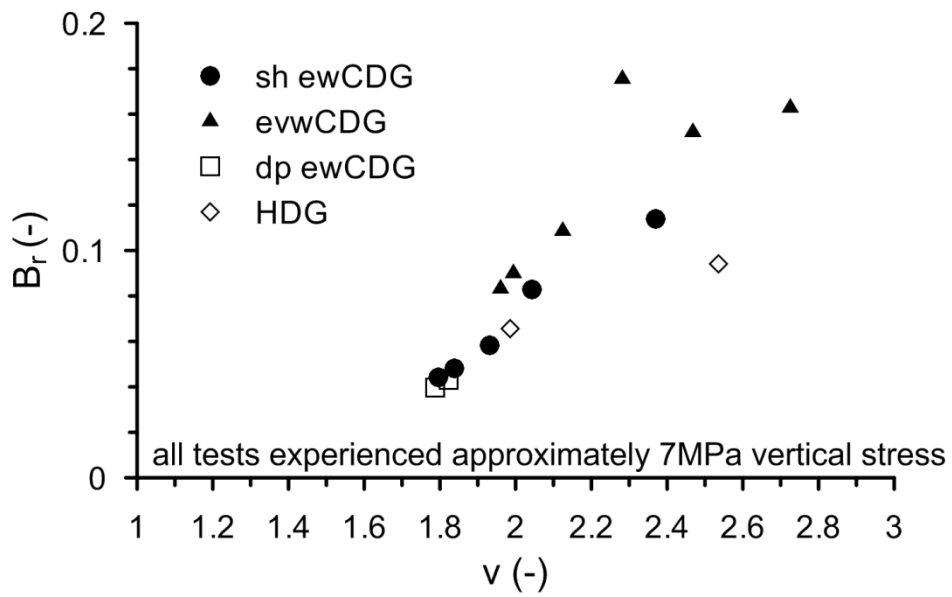




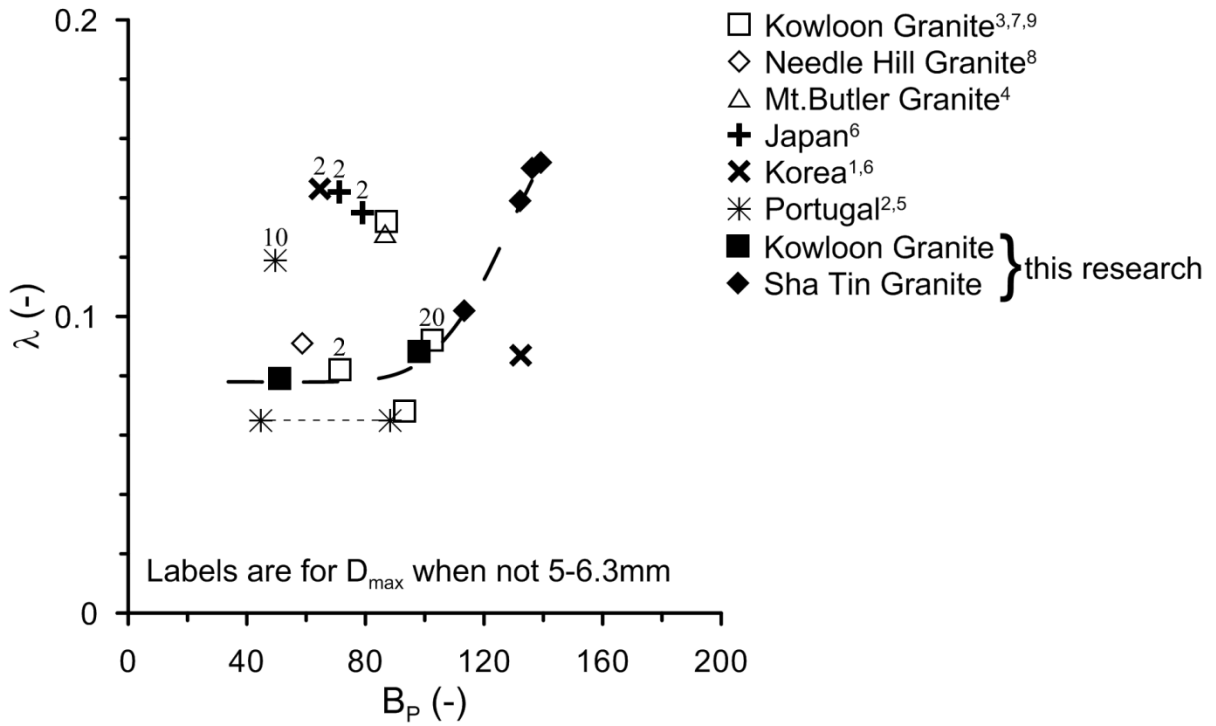
**Fig.7** Trend of compressibility with coefficient of uniformity: (a) NCL slope and (b) NCL intercept. <sup>1</sup> Lee & Coop (1995), <sup>2</sup> Viana da Fonseca (1998), <sup>3</sup> Fung (2001), <sup>4</sup> Ng & Chiu (2003), <sup>5</sup> Viana da Fonseca et al. (2006), <sup>6</sup> Ham et al. (2010), <sup>7</sup> Zhang (2011), <sup>8</sup> Yan & Li (2012) and <sup>9</sup> Madhusudhan & Baudet (2014)



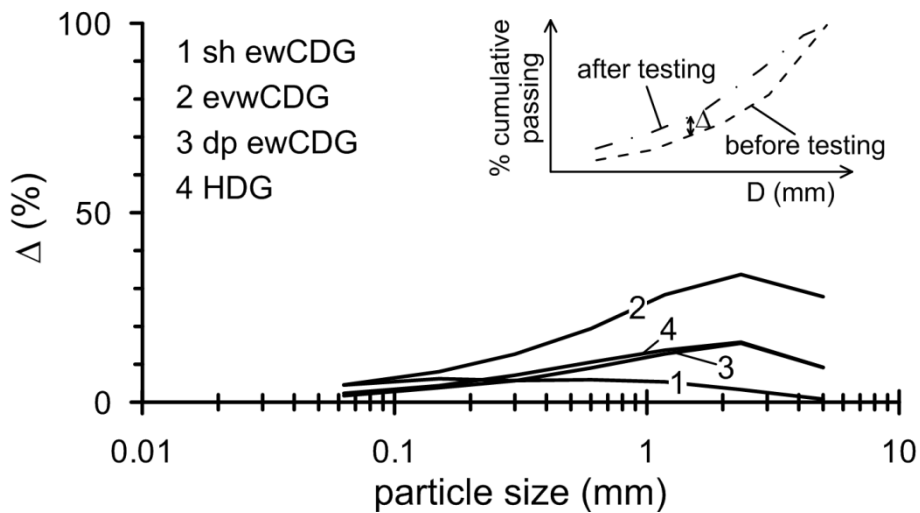
**Fig.8** Particle breakage for the soils studied in this research. Trend with vertical stress



**Fig.9** Particle breakage for the soils studied in this research. Trend with specific volume



**Fig.10** Trend of compressibility with breakage potential. <sup>1</sup> Lee & Coop (1995), <sup>2</sup> Viana da Fonseca (1998), <sup>3</sup> Fung (2001), <sup>4</sup> Ng & Chiu (2003), <sup>5</sup> Viana da Fonseca et al. (2006), <sup>6</sup> Ham et al. (2010), <sup>7</sup> Zhang (2011), <sup>8</sup> Yan & Li (2012) and <sup>9</sup> Madhusudhan & Baudet (2014)



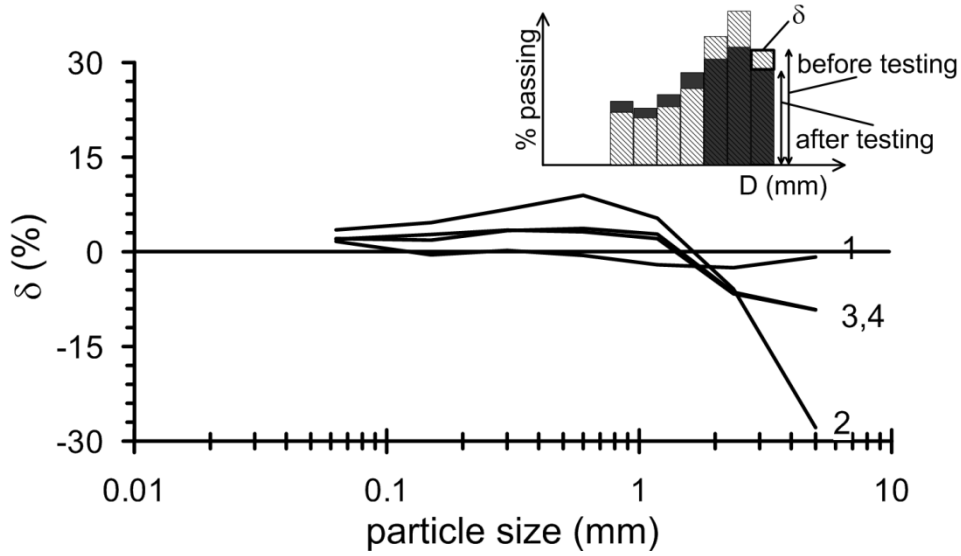


**Fig.11** Change in the grading components as a result of breakage: (a) cumulative curves and (b) histograms

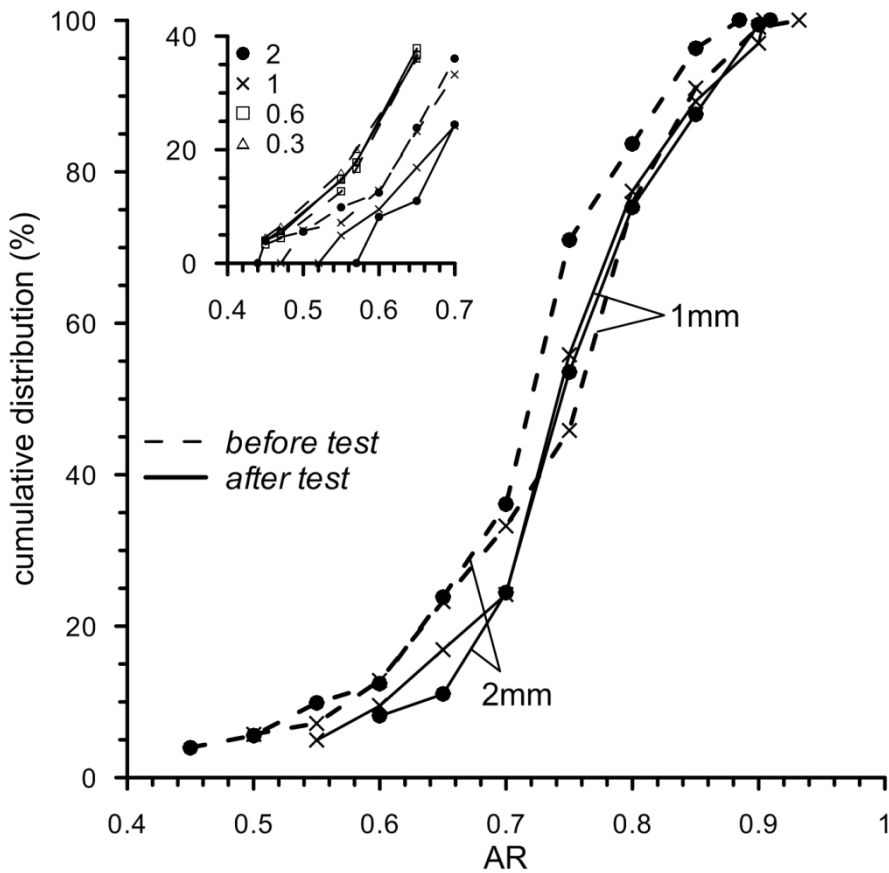


**Fig.12** Change in the particle morphology as a result of breakage: (a) aspect ratio and (b) convexity

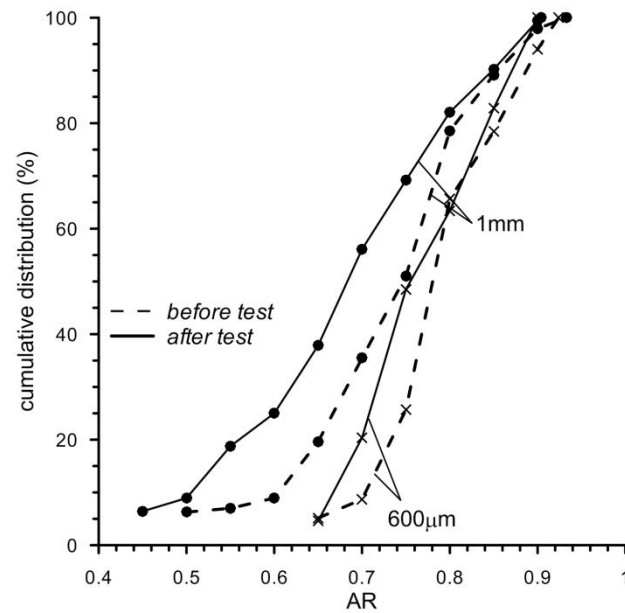
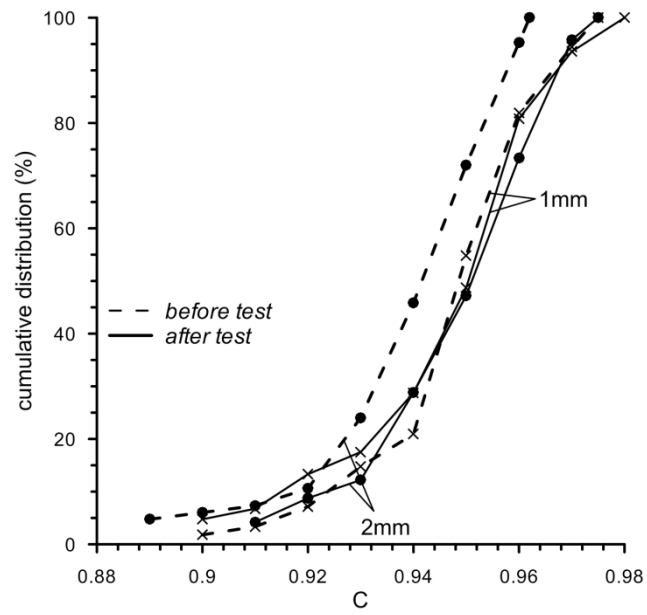


**Fig.13** Change in the particle morphology as a result of breakage for the sh ewCDG.